Dynamic characteristics of impact-induced brain strain in the corpus callosum

Songbai Ji [1, 2 *], Shaoju Wu [1], Wei Zhao [1]

[1] Department of Biomedical Engineering, Worcester Polytechnic Institute, Worcester, MA

[2] Department of Mechanical Engineering, Worcester Polytechnic Institute, Worcester, MA

[*] Corresponding author:

Dr. Songbai Ji

60 Prescott Street

Department of Biomedical Engineering

Worcester Polytechnic Institute

Worcester, MA 01506, USA

sji@wpi.edu; (508) 831-4956

Resubmitted to the *Brain Multiphysics*, February 1, 2022

Abstract

Impact-induced brain strains are spatially rich and intrinsically dynamic. However, the dynamic information of brain strain is not typically used in any injury investigation. Here, we study the dynamic characteristics of maximum and minimum principal strain (maxPS and minPS) of the corpus callosum and highlight the significance of impact simulation time window. Three datasets are used: laboratory reconstructed National Football League (NFL; N=53), measured impacts from Stanford (SF; N=110) and Prevent Biometric (PB; N=314). Impact cases are discarded (by 20.8%, 11.8%, and 66.2%, respectively), when the simulation time window is considered inadequate to capture sufficient strain temporal responses. Fitted Gaussian peaks (with average relative root mean squared error of ~5% and R^2 >0.9) from all datasets have a similar median (15–18 ms) and inter-quantile range (5–9 ms) for the full width at half maximum (FWHM). FWHM significantly and negatively correlates with strain magnitude for NFL and SF, but not for PB. However, ratios between the largest minPS and maxPS magnitudes are similar across datasets (median of 0.5–0.6 with inter-quantile range of 0.2–0.7). Dynamic strain features improve injury prediction. This study motivates further development of advanced deep learning models to instantly estimate the complete details of spatiotemporal history of brain strains, beyond spatially detailed peak strains obtained at maximum values currently available. In addition, this study highlights the time lag between impact kinematics and corpus callosum strain deep in the brain, which has important implications for impact simulation and result interpretation as well as impact sensor designs in the future.

Keywords: traumatic brain injury; dynamic characteristics; Gaussian peak; full width at half maximum (FWHM); Worcester Head Injury Model (WHIM)

Introduction

Traumatic brain injury (TBI) has been called "the most complicated disease of the most complex organ of the body" (Marklund and Hillered 2011) and is an increasingly high-profile public health issue (Kenzie et al. 2017). Blunt TBI is the result of mechanical insult to the brain induced by external head impact. It is now well accepted that brain mechanical responses such as strain and stress, rather than peak linear and/or rotational acceleration, is the direct cause of brain injury (King et al. 2003; Meaney et al. 2014; Fahlstedt et al. 2021). Due to the near incompressibility property of the brain, linear acceleration leads to little strain, as verified in several head injury models (Kleiven 2007; Ji et al. 2014; Bian and Mao 2020). In contrast, head rotation plays the primary role in inducing brain strain, which is consistent with recent efforts in developing various rotational kinematics-based injury metrics (Gabler et al. 2018; Bian and Mao 2020).

Historically, brain strain has been characterized by the peak maximum principal strain (maxPS) of the whole brain from impact simulation using a computational head injury model. This scalar numeric value quantifies the peak magnitude of tissue stretch in a three-dimensional (3D) space, regardless of the anatomical location, stretch direction, or time of occurrence. MaxPS remains in wide use and currently serves as a benchmark to measure the quality of numerous kinematics-based injury metrics (Gabler et al. 2018; Bian and Mao 2020).

However, maxPS of the whole brain grossly oversimplifies the brain biomechanical responses. First, it does not inform the anatomical location of where the peak strain occurs. Effectively, it treats the entire brain as a single unit, which lacks spatial resolution in correlating with detailed pathology of brain injury such as those observed in neuroimages (Bigler 2016). Second, the direction of maxPS does not (necessarily) correspond to that of the stretch along white matter fiber tracts based on which injury thresholds in terms of magnitudes of axonal strain and/or strain rate are typically established (Morrison et al. 2011). Studies have identified significant disparities between maxPS and strain along white matter fibers (Giordano and Kleiven

2014; Ji et al. 2015), which highlight the potential deficiency in using maxPS for injury correlation in the white matter.

There have been ongoing efforts to extend maxPS of the whole brain to regional maxPS such as those in the gray/white matter, corpus callosum, mid-brain, brainstem, and other sub-regions of the brain (Viano et al. 2005; Kleiven 2007; McAllister et al. 2012; Post et al. 2017; Bian and Mao 2020). Recently, efforts have extended to the entire 50 deep white matter regions (Zhao et al. 2017) and 129 gray matter areas (Anderson et al. 2020). Orientation-dependent strains along white matter fiber directions have also been proposed to study the mechanism of injury (Giordano and Kleiven 2014; Ji et al. 2015; Sahoo et al. 2016; Wu et al. 2019b; Garimella et al. 2019; Li et al. 2020). A recent network-based injury metric further extends these efforts by sampling both regional maxPS in isotropic gray matter areas as well as their interconnecting white matter fiber strains for injury prediction (Wu et al. 2020). A theoretical framework has also been established to comprehensively delineate white matter tract-related deformation (Zhou et al. 2021), which can be made much more efficient and accurate using a voxelized relative brain-skull displacement field (Ji and Zhao 2022). These regional and direction-specific strains exploit the richness in brain strain spatial distribution that generic maxPS of the whole brain is unable to offer.

Nevertheless, brain strain is not only spatially rich but also intrinsically dynamic. For the vast majority of TBI incidents including mild TBI where no macroscopic tissue tear occurs or is expected, it is reasonable to assume that brain strain would start from zero and return to zero after impact. Most injury studies use peak, positive principal (Viano et al. 2005; Kleiven 2007; McAllister et al. 2012; Post et al. 2017; Bian and Mao 2020) or fiber strain (Giordano and Kleiven 2014; Ji et al. 2015; Sahoo et al. 2016; Wu et al. 2019b; Garimella et al. 2019; Li et al. 2020) over the entire impact duration to evaluate the risk of injury. This implies that tissue experiencing the same peak positive strain will have an identical risk of injury, irrespective of whether they experience tension only or both tension and compression, sustain different strain rates (Morrison et al. 2011; Bar-Kochba et al. 2016), or have different temporal exposure to above-threshold strains, as illustrated in **Fig. 1** for four hypothetical scenarios.

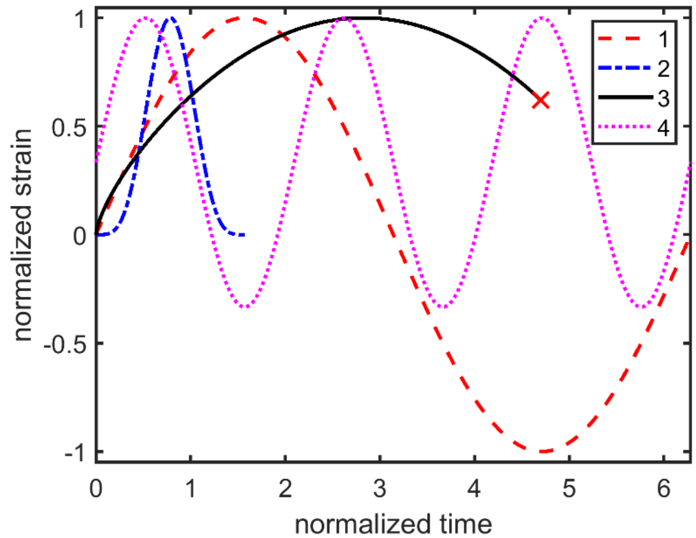

Fig. 1. Illustration of four hypothetical strain response time histories. All history curves have the same peak strain magnitude. This would imply an identical risk of injury based on the current practice, even though they may experience single (1, 2, and 3) or multiple (4) strain cycles, tension only (2 and 3) vs. tension and compression (1 and 4), or of different strain rates that lead to shorter (2) or longer (3) exposure to above-threshold strains. Although strain is expected to start from zero and return to zero in a realistic head impact for the vast majority of TBI incidents, it is possible that only an incomplete strain history is available (e.g., case #3) due to limited time window for impact simulation.

It is known that strain rate plays a critical role in neuronal injury (Morrison et al. 2011; Bar-Kochba et al. 2016). Combining strain and strain rate (e.g., using their product (King et al. 2003)) would somewhat mitigate the lack of consideration of the strain history, beyond peak strain magnitude alone. However, this is still not sufficient to address the uncertainty of the risk of injury related to whether both positive and negative strains are experienced, or the number of strain peaks sustained (**Fig. 1**). More fundamentally, current model-based TBI studies generally do not consider the dynamic brain strain time history but this is critical when using it as input to drive a microscale, axonal injury model (Montanino et al. 2021). In addition, little attention has been paid to the negative, compressive strains (with few recent exception (Miller et al. 2021)), even though they are also injury-causing as observed in *in vitro* neuronal injury studies (Bar-Kochba et al. 2016).

Therefore, the primary purpose of this study is to investigate the dynamic characteristics of impact-induced brain strain. Previous studies have investigated the dynamics of relative brain-skull displacement or strain in the frequency domain (Laksari et al. 2015; Abderezaei et al. 2019; Mojahed et al. 2020; Escarcega et al. 2021). Here we report dynamic characteristics of brain strain in the temporal domain. We focus on maxPS and the negative, minimum principal strain (minPS; 1st and 3rd principal strains, respectively) in the mid-sagittal section of the corpus callosum as this region is known to be vulnerable both biomechanically (Kleiven and Hardy 2002; Zhao et al. 2017; Hernandez et al. 2019) and in neuroimaging (Bigler and Maxwell 2012). In addition, limiting the investigation to a specific region eliminates a potential confounding factor when comparing findings across impacts. Quantifying the global strain dynamic characteristics of the corpus callosum may facilitate downstream microscale axonal injury model simulations in this region (Montanino et al. 2021), e.g., by eliminating the need for a costly global model simulation. This may be especially important when there is a need to consider the cumulative effects from many head impacts that require high throughput in model simulations.

As a secondary goal, we also investigate whether impact simulation using the given kinematic loading profile is sufficient to characterize dynamic strains in the corpus callosum. Given the unique material properties of the brain, it takes finite amount of time for the stress wave initiated at the brain-skull boundary to propagate into this anatomical region deep in the brain. Therefore, it is possible that corpus callosum strain may not have reached its peak even if the input kinematics capture the peak rotational acceleration or velocity. A recent study investigates the minimum time window required for impact simulation by comparing simulated peak strains of the whole brain using truncated kinematic profiles with those obtained from the original (Liu et al. 2021). However, it used the 95^{th} percentile peak MPS and its rate of the whole brain, which do not inform the anatomical region where the peak strain/strain rate occurs. The importance of sufficient impact time window for simulation was similarly noted in another study, where only 36 out of the 53 reconstructed NFL head impacts were retained by examining whether maximum strains were reached within the provided load trace duration (Zhou et al. 2021). In this study, again, we focus on the mid-sagittal section of the corpus callosum to mitigate a confounding factor resulting from the uncertainty in anatomical location where peak strain occurs.

Findings from this study may contribute towards a comprehensive understanding of the spatiotemporal dynamics of brain strain. In addition, the significance of impact simulation time window may have some practical implications on impact simulation and result interpretation in general, as well as impact sensor designs in the future.

Methods

Impact datasets

We employed three impact datasets for analyses in this study: head kinematics generated by laboratory reconstructions of professional football helmet impacts (NFL; N=53) (Sanchez et al. 2018), measured on-field head impacts from a variety of contact sports at Stanford University (SF; N=110) (Hernandez et al. 2015) and from Prevent Biometrics (PB; N=314) (Zhao et al. 2019) using mouthguards. These datasets were previously used to train and test deep learning models for rapid strain estimation with high accuracy (Wu et al. 2019a; Ghazi et al. 2021).

All datasets provide time-varying linear acceleration and rotational velocity profiles relative to the head center of gravity. For each NFL impact case, we used the prescribed impact duration that is considered "valid" (Sanchez et al. 2018) and further trimmed the initial time period of essentially zero rotational velocity magnitude. This helped decrease the impact simulation runtime without inducing any difference in strain. The average length of temporal window of recorded non-zero kinematic profiles for the NFL dataset was 88±63 ms (range of 18–240 ms). In comparison, the temporal length for the SF and PB datasets were fixed to 97 ms and 50 ms, respectively. The temporal resolutions for the NFL, SF and PB were 0.1 ms, 1.0 ms, and 0.31 ms, respectively. They were all resampled at 1 ms temporal resolution, as required by the previous deep learning models by design (Wu et al. 2019a; Ghazi et al. 2021). The impact datasets are summarized in **Fig. 2** in terms of peak rotational and linear accelerations vs. velocity magnitudes.

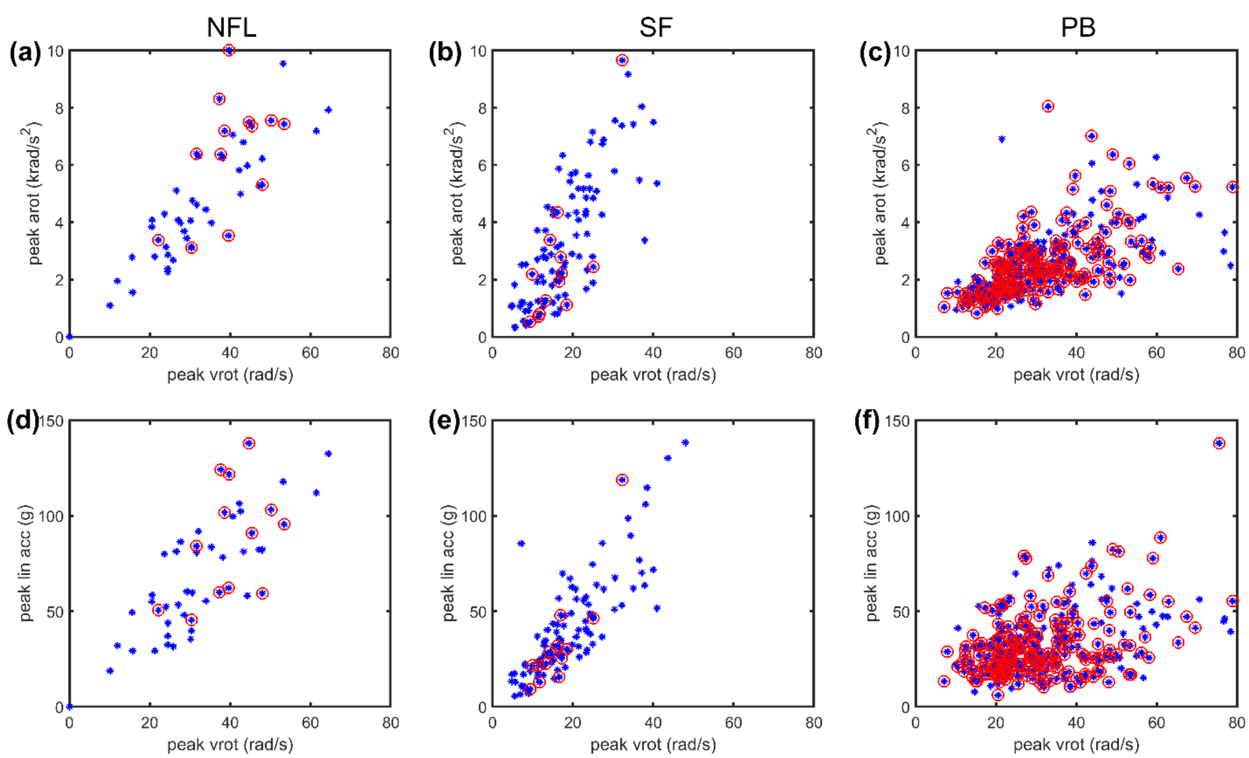

Fig. 2. Summary of peak rotational acceleration (arot) vs. peak rotational velocity (vrot; top) and summary of peak linear acceleration vs. vrot for the NFL (**ad**), SF (**be**), and PB (**cf**) datasets. Circles indicate discarded cases (by 20.8%, 11.8%, and 66.2%, respectively, for the three

datasets) because their time windows were considered not sufficient to completely capture the temporal responses of either maxPS or minPS in the corpus callosum (explained in next section).

Impact simulations and exclusion criterion

The three impact datasets were previously simulated using the anisotropic Worcester Head Injury Model (WHIM) V1.0 (Zhao and Ji 2019) when developing our deep learning models (Wu et al. 2019a; Ghazi et al. 2021). The WHIM V1.0 was recently validated against a wide range of blunt impact conditions, achieving a peak strain ratio (simulation vs. experiment) of 0.94±0.30 based on marker-based strains from 12 high/mid-rate cadaveric impacts and reasonable agreement with strains from four low-rate *in vivo* head motions (Zhao and Ji 2020a). A ratio of 1.00±0.00 relative to experimental strains would be "perfect", although errors from experimental strains, themselves, should not be ignored (Zhao et al. 2021). The head coordinate system was chosen such that the posterior-to-anterior, right-to-left, and inferior-to-superior directions corresponded to the *x*, *y*, and *z* directions, respectively. The simulation time window was identical to the corresponding impact duration from the given head impact kinematics. These simulations provided time history curves for maxPS and minPS for every brain element across all time frames (at a resolution of 1 ms). In this study, we focused the analyses on the corpus callosum strains.

Due to the brain's near incompressibility property, only head rotational velocity profiles (transformed into a ground-fixed coordinate system to decouple head translational and rotational motions (Wu et al. 2021)) were used for impact simulation. This was because linear acceleration produces little strain for the majority of the brain, including the corpus callosum, as confirmed by several head injury models, including the WHIM (Kleiven 2007; Ji et al. 2014; Bian and Mao 2020). This strategy allowed to substantially reduce the input parametric space, and hence, the number of training samples required to achieve high accuracy with a deep learning model (Wu et al. 2019a; Ghazi et al. 2021). Linear acceleration does influence brain strain in the brainstem/foramen magnum region for the WHIM when there is a large acceleration component along the superior-to-inferior direction, which can be compensated for to further improve accuracy (Wu et al. 2021). Regardless, linear acceleration has virtually no effect on the corpus callosum strain analyzed in this study.

For each simulated impact, the element within the mid-sagittal section of the corpus callosum that experienced the highest maxPS across all time frames was identified. Similarly, the element experienced the lowest minPS value across all time frames was also identified, which may not be the same as that to experience the highest maxPS. Nevertheless, for each dataset across all impacts, the identified elements were rather similar in location between maxPS and minPS. They were also similar across the three impact datasets (**Fig. 3**).

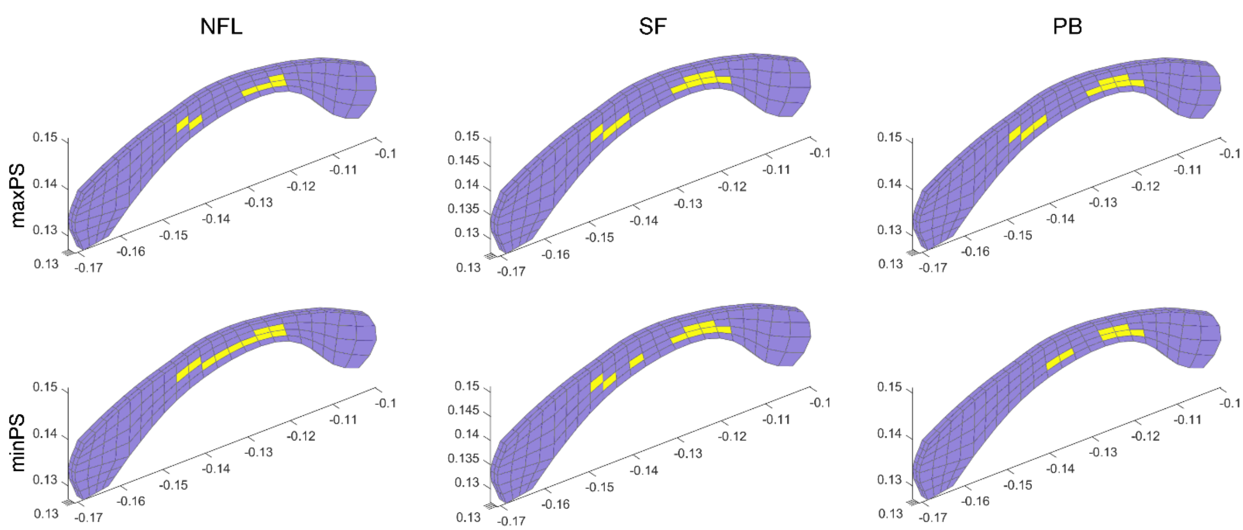

Fig. 3. Across all impacts for the three datasets, the elements identified as having experienced the highest maxPS (top) or lowest minPS (bottom) are highlighted. They are clustered in a limited region and are rather similar between the two strain measures and across the three impact datasets. Coordinate system in meters.

No numerical artefacts were detected for either maxPS or minPS time histories, as compared to the those of their neighboring elements. For all peaks, the magnitude differences relative to those of the immediate neighboring elements were <5%, along with a correlation coefficient >0.95 (using a temporal window of 20 ms centered at the peak). **Fig. 4** illustrates maxPS time histories of all corpus callosum elements for a typical impact for each dataset.

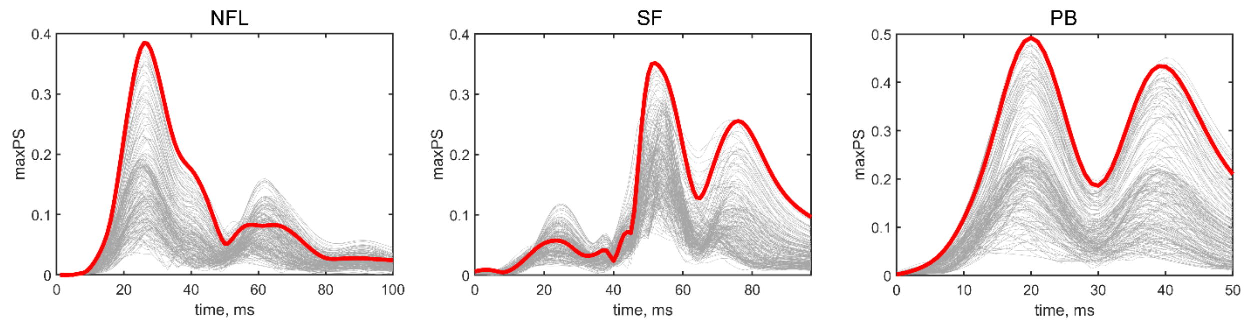

Fig. 4. Illustration of maxPS time histories of corpus callosum elements in typical NFL, SF, and PB impact, with the one experiencing the highest maxPS highlighted. No obvious artifacts were detected. The same is true for minPS, which is not shown for brevity.

For any impact, if the maximum magnitude of maxPS or minPS did not peak within the time window, or the peak occurred but it was too close to the right end of the impact window (<5 ms), it was considered not enough to completely capture the strain temporal response to ensure a robust Gaussian peak fitting, see next section. Therefore, it was discarded from subsequent analyses of the corresponding strain measure (but not necessarily excluded for the other strain). This was justified because any strain is expected to start from zero and return to zero after impact (assuming the tissue continuum remains without residual strain). **Fig. 5** shows example cases that were discarded.

Peak identification and analytical fitting

For a given maxPS and negative minPS strain history curve, the peak with the largest magnitude was first identified. Some impacts also led to significant secondary strain peaks (e.g., minPS for the SF impact in **Fig. 5**). Secondary peaks that had a magnitude at least 50% of the largest peak with a minimum peak prominence or vertical drop of at least 10% of the largest peak value were also identified, if they existed. Visual inspections of the hundreds of peaks revealed that they typically resembled a "bell shape". This inspired us to fit them into an analytical Gaussian form to facilitate analysis, which has been extensively used in other fields (e.g., in chromatography (Kalambet et al. 2011; Wahab and O'Haver 2020) and chemistry (Mittermayr et al. 1996)). A Gaussian peak is defined by a mathematical form of:

$$f(x) = a \times exp\left(-\frac{(x-b)^2}{2c^2}\right), \quad (1)$$

where a is the height of the curve's peak, b is the peak center position, and c is the standard deviation. A more commonly used measure of the Gaussian peak is the full width at half maximum (FWHM) that quantifies the curve width at points on the *y*-axis that are half the maximum amplitude (O'Haver 2021). It is effectively ~2.355 times c.

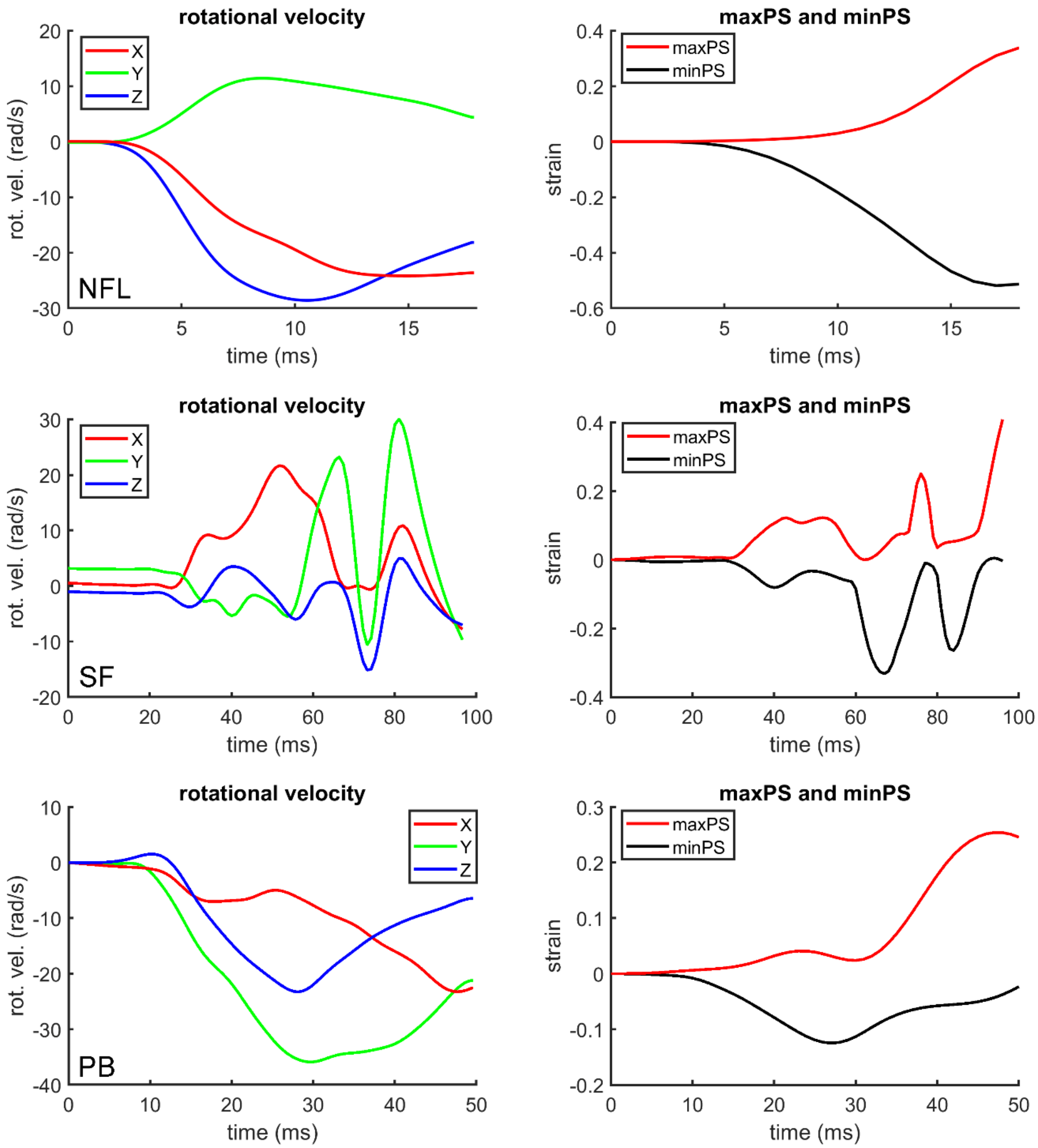

Fig. 5. Examples of discarded cases showing the head rotational velocity profile and the corresponding maxPS and minPS time histories for the three impact datasets. The example NFL impact was excluded for both maxPS and minPS analyses. The example SF and PB impacts were both excluded for maxPS analysis but not for minPS analysis. Although maxPS achieved its peak in the PB case, its occurrence was too close to the temporal window boundary (within the empirical threshold of 5 ms) to allow robust Gaussian peak fitting.

The identified peaks were separately fitted into a Gaussian peak (O'Haver 2021) centered at the identified peak locations with a window size of 20 ms. The window size was empirically determined with trial and error. The fitting quality was assessed by fitting errors in terms of relative root mean squared error (RMSE divided by the mean of observed values) and coefficient of determination (R^2) (O'Haver 2021).

Concussion prediction

An ultimate use of model simulation is to predict the occurrence of injury. Therefore, we examined whether combining additional information from strain dynamics in the corpus callosum can improve injury prediction performance. The NFL dataset was used for this purpose. This dataset has 20 concussions and 33 non-injury cases, and it has been widely used to assess the performance of concussion prediction (Wu et al. 2020; Zhou et al. 2021). The other two datasets were not used, as they had too few or no injury cases to allow such an evaluation. To maximize the use of all impacts for injury prediction, an additional 20 ms beyond the recorded temporal window (padded with zero rotational acceleration (Ghazi et al. 2021)) were used for impact simulation. This ensured that both maxPS and minPS in the corpus callosum have reached their peak values.

First, we employed peak maxPS in corpus callosum alone for concussion prediction using feature-based support vector machine (SVM). Baseline performances including accuracy, sensitivity, specificity, and positive predictive value were obtained *via* a leave-one-out cross-validation framework, as conducted before (Wu et al. 2020). Specifically, one case was used for testing based on the trained model using all the remaining cases. This process was repeated until all cases were predicted for injury for exactly once, from which the performance was evaluated. Next, we combined both peak maxPS and minPS, and further adding their corresponding peak strain rate magnitudes (as produced from model simulation) for concussion prediction. The same SVM and cross-validation framework were used for performance evaluation.

Data analysis

All impact simulations were conducted previously using Abaqus/Explicit (Version 2018; Dassault Systèmes, France) on a Linux cluster (Intel Xeon E5-2680v2, 2.80 GHz, 128 GB memory). For each impact dataset, we reported the characteristics of fitted Gaussian peaks for maxPS and minPS in terms of the FWHM. Its association with respect to strain magnitude was also analyzed using Pearson correlation. For impact cases retained for both maxPS and minPS analyses, the ratio between their respective highest peak magnitudes within the simulation time window were also reported. Statistical significance was reached when $p<0.05$. Finally, injury prediction performances from leave-one-out cross-validations were compared. All data analyses were conducted in MATLAB (R2020a; Mathworks, Natick, MA).

Results

Table 1 summarizes the fitting quality of the Gaussian peaks, along with the percentage of discarded cases and the percentage of retained cases that had secondary peaks for the two strain measures from the three impact datasets.

Table 1. Summary of Gaussian peak fitting errors (root mean squared error relative to the mean and R^2), the percentage of cases that had to be discarded from relevant analysis (% discarded), the percentage of retained impacts that more than one peak was identified (% secondary), and the percentage of discarded cases when analyzing the ratio between minPS and maxPS magnitudes (% discarded for both, as both are necessary to compute the ratio). The corresponding numbers of discarded cases are also shown in parentheses.

	Relative RMSE	R^2	% discarded	% secondary	% discarded for both
NFL maxPS	4.2±3.3%	0.95±0.08	9.4% (5)	47.2% (25)	24.5% (13)
NFL minPS	4.9±3.9%	0.93±0.11	17.0% (9)	43.4% (23)	
SF maxPS	5.2±4.3 %	0.93±0.11	3.6% (4)	24.5% (27)	11.8% (13)
SF minPS	7.2±5.5%	0.87±0.19	8.2% (9)	46.6% (51)	
PB maxPS	2.4±2.0%	0.98±0.06	31.8% (100)	1.3% (4)	66.2% (208)
PB minPS	4.4±4.9	0.91±0.26	38.2% (120)	11.3% (35)	

For cases that were retained for analysis, **Fig. 6** reports the strong linear relationships between maxPS/minPS and the peak resultant rotational velocity magnitude. The regression slopes were largely similar across datasets, especially between NFL and SF, which also had an improved fitting quality in terms of RMSE compared to PB. **Fig. 7** shows typical maxPS and minPS peaks overlaid with their fitted Gaussian peaks, along with their corresponding rotational velocity profiles for each impact dataset.

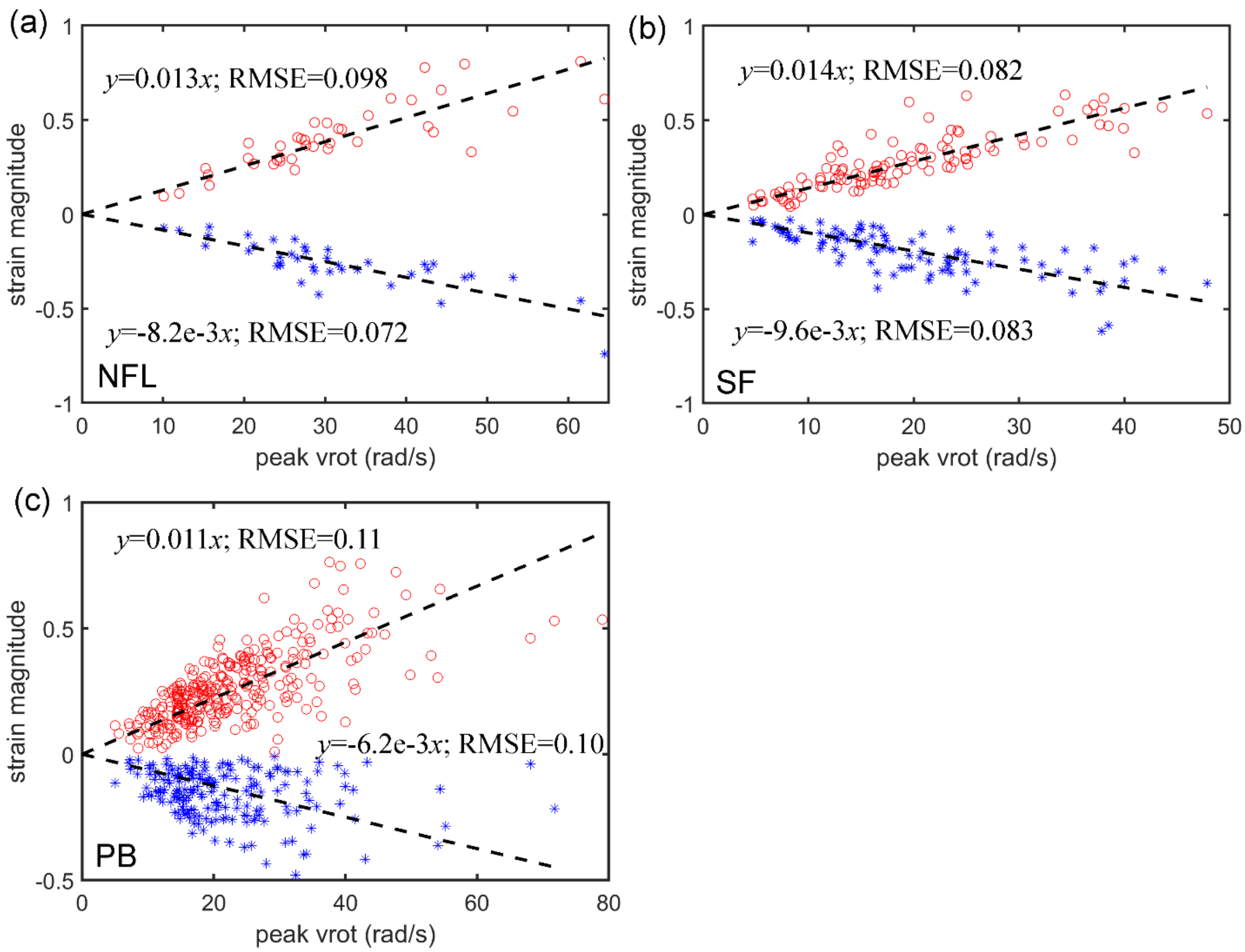

Fig. 6. Summary of maxPS (circles, positive) and minPS (stars, negative) relative to the peak resultant rotational velocity (vrot) for the three impact datasets, NFL (**a**), SF (**b**), and PB (**c**). Only cases that are retained for analysis are shown for each strain. Both maxPS and minPS are significantly associated with the peak vrot magnitude (p<0.001). Linear regression fitting results with zero intersect are also shown, along with the fitting root mean squared error, RMSE.

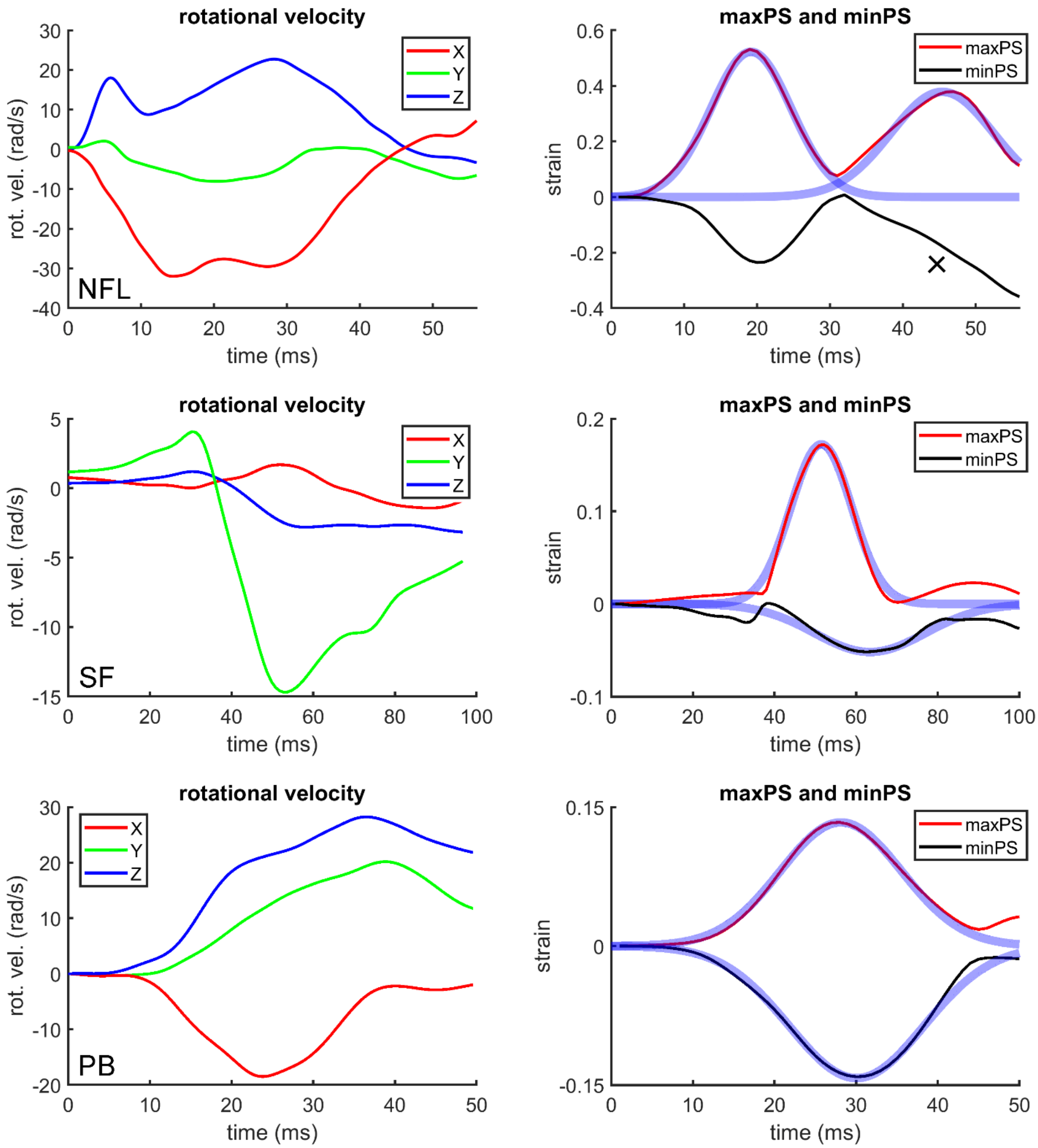

Fig. 7. Selected cases from the three impact datasets to compare the head rotational velocity profile and the corresponding maxPS and minPS. The fitted Gaussian peaks are overlaid. Two peaks of maxPS in the NFL case are successfully fitted, but the case is discarded for minPS analysis because it did not reach the maximum peak.

Fig. 8 summarizes FWHM values from fitted Gaussian peaks. For both strain measures, the medians and inter-quantile ranges were similar across impact datasets (15–18 ms and 5–9 ms, respectively). For the NFL and SF datasets, FWHM was significantly and negatively associated with the magnitudes of maxPS and minPS peak values (Pearson correlation coefficient range from –0.41 to –0.44, and from –0.29 to –0.22, respectively; $p<0.001$), but not for the PB dataset ($p=0.5$).

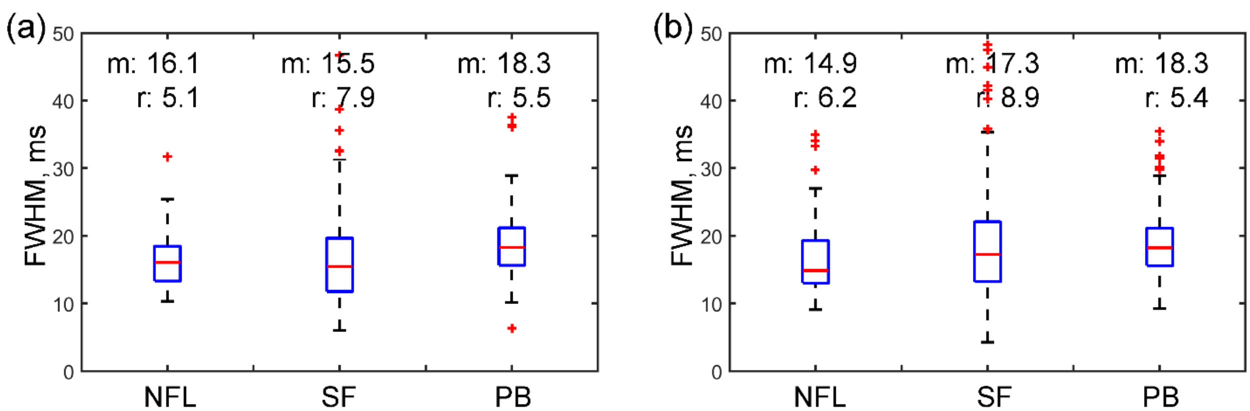

Fig. 8. Boxplots summarizing the FWHM (in ms) for the fitted Gaussian peaks of maxPS (**a**) and minPS (**b**) for the three impact datasets. The median (m) and inter-quantile range (r) are also reported.

Fig. 9 reports the ratio between minPS and maxPS magnitudes across the three datasets. Again, they had a similar median (0.5–0.6), although the inter-quantile range for the PB was notably larger (0.75 vs. 0.23–0.38 for NFL/SF).

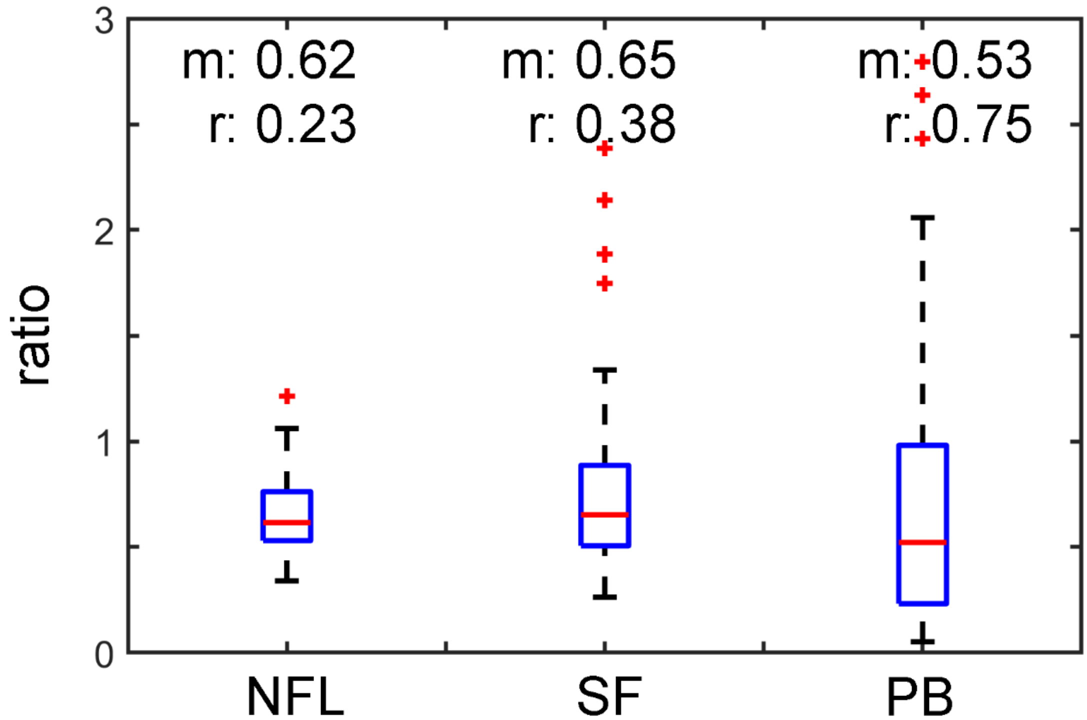

Fig. 9. Boxplots summarizing the ratios between the largest minPS and maxPS magnitudes within the simulated time window for the three impact datasets. The median (m) and inter-quantile range (r) are also reported.

Finally, the injury prediction performances when using peak maxPS alone (as commonly adopted), combining peak maxPS and peak minPS, as well as further combining their corresponding peak strain rate magnitudes are compared (**Table 2**). With every additional feature(s) added, injury prediction performances consistently improved across all measures using the objective leave-one cross-validation procedure.

Table 2. Comparison of injury prediction performances in terms of accuracy, sensitivity, specificity, and positive predictive value based on the NFL dataset when using peak maxPS alone, peak maxPS and peak minPS, as well as further combining their peak strain rate magnitudes.

	peak maxPS	peak maxPS and peak minPS	peak maxPS, peak minPS, and their peak strain rates
Accuracy	0.642	0.698	0.774
Sensitivity	0.250	0.300	0.500
Specificity	0.879	0.934	0.934
Positive predictive value	0.556	0.750	0.833

Discussion

Whenever the head changes its angular orientation in space during impact, a shear stress wave is continuously initiated at the brain-skull interface, which travels towards the center of the brain and interacts with all previously generated waves. This leads to complex dynamic deformation of regional brain tissue that experiences tension, compression, shear, and torsion. The brain's viscoelasticity along with the low shear modulus and high bulk modulus causes a lag between the skull rotational kinematics and strain in the corpus callosum deep in the brain. Therefore, there is a rich time history of the dynamic brain strain, beyond the richness in its spatial distribution. Although brain strain dynamics are readily available from impact simulation, they are not yet typically used in any injury investigation.

Based on hundreds of real-world head impacts from three different sources, we found both maximum and minimum principal strains (maxPS and minPS, respectively) in the corpus callosum can experience one or more peaks within the captured time window. Each resembled a “bell” shape that can be approximated into a Gaussian peak. From all impacts in the three datasets, the FWHM values were rather similar in median (15–18 ms) and inter-quantile range (5–9 ms). In general, peak minPS magnitudes were lower than those of maxPS, with a median ratio consistently of 0.5–0.6 across the three datasets.

The “bell” shape of maxPS response history has been observed in previous studies simulating typical NFL impacts, with either a single peak (Viano et al. 2005; Kleiven 2007) or a pair of major peaks (Kleiven 2007) across the impact duration. However, the earlier studies did not specifically report the associated anatomical locations, which prevented a direct comparison with the findings in the corpus callosum in the current study. A more recent study also reported single peaks of maxPS in different corpus callosum subregions when simulating a head impact from the SF dataset (Montanino et al. 2021), albeit somewhat more complicated with minor peaks as well (vs. mostly smooth here and in previous studies (Viano et al. 2005; Kleiven 2007)). These largely consistent observations across different impact datasets and diverse head injury models corroborate the quantitative findings reported here based on the anisotropic WHIM V1.0.

A potential application utilizing the Gaussian peak parameters is to establish simplified but realistic strain time history to design *in vitro* neuronal tissue injury experiments that are more closely related to real-world injury (Bar-Kochba et al. 2016), or to drive microscale axonal injury models (Montanino et al. 2021). Until most recently (Montanino et al. 2021), deformation of axonal injury models has been driven by assumed loading conditions such as a representative and fixed strain magnitude at a fixed strain rate (Ahmadzadeh et al. 2014; Montanino et al. 2019; Alisafaei et al. 2020). These assumed loading conditions do not reflect the variable strain rate and do not have an unloading phase that must happen in the real world. Thus, they may not truly reflect a biofidelic loading condition. Nevertheless, it should be noted that the maxPS and minPS analyzed here still do not inform a specific direction of strain, such as along the white matter fiber tract. This is a limitation of the current study, which suggests the need for continual investigation into brain strain dynamic characteristics along the white matter fibers. Work is currently underway to calculate dense white matter fiber strains of the entire tractography with sufficient accuracy and efficiency (Shakiba et al. 2020), which will be utilized in the future.

The strain dynamic characteristics can also serve as response "features" to enable machine learning methods such as SVM for injury correlation and prediction (vs. univariate logistic regression commonly used). Compared to using peak maxPS alone, adding additional "features" such as peak minPS and their peak rate magnitudes consistently improved injury prediction performances (**Table 2**). However, the performance was notably poorer than when using a network-based injury metric (Wu et al. 2020), as the latter was based on strain of the whole brain (e.g., maximum positive predictive value of 0.833 here vs. 0.938). This suggests the potential of extending the dynamic characterization to the whole brain strain, not just the corpus callosum in this study. Nevertheless, it is important to note that conventional injury "correlation" does not (necessarily) inform injury "causation". A large-scale axonal injury modeling framework may have the potential to uncover the underlying injury pathology in axonal substructural damages (Johnson et al. 2013). The dynamic characteristics of brain strain investigated here would set the stage to facilitate such an effort in the future.

Finally, we also observed that the three impact datasets had significantly different percentages of impacts considered insufficient to capture corpus callosum peak strains (from 11.8% for SF to 66.2% for PB; **Table 1**) as they either did not reach peak or occurred too close to the time window border (**Fig. 5**). Even if impact kinematics have captured the peak magnitudes of head rotational velocity, they may still not be enough for corpus callosum to reach peak strain due to the time lag resulting from the brain's viscoelasticity. For the PB and SF datasets with the shortest and longest impact time window, respectively, they also had the most and fewest cases considered insufficient for the time window, respectively (**Table 1**).

To further quantify the time lag, we used idealized head rotational impulses for investigation. A head rotational acceleration impulse of a triangular shape (peak rotational acceleration of 4500 rad/s^2) was imparted separately along the three major anatomical axes (Ji and Zhao 2015). The resulting maxPS had varying time-to-peak values, ranging from 5 ms to 16 ms (for sagittal and axial rotation, respectively) relative to the rotational acceleration peak (**Fig. 10**). When the magnitude of head rotational acceleration was reduced (to 1500 rad/s^2), the time-to-peak further delayed to 23 ms for the axial impulse. The elongated peak temporal shape was consistent with the earlier finding that FWHM significantly and negatively correlated with strain peak magnitude.

These results could provide important insight into the minimum time window required for head impact sensors (Sanchez et al. 2018; Liu et al. 2020, 2021). Not only do they need to capture the maximum head rotational kinematics (**Fig. 5** and **Fig. 7**), but they also need to consider at least ~20 ms additional time for the deep brain to reach peak strain. When absent, it is recommended to simulate an additional ~20 ms (e.g., by assuming a zero acceleration at the end of impact window), which could mitigate the issue and "rescue" the recorded impacts. This is confirmed for all the three discarded example cases in **Fig. 5**. This was also the reason that the previous pre-computed brain response atlas (pcBRA) had an additional 23 ms impact simulation beyond the peak acceleration (or, 18 ms after velocity reached its peak; **Fig. 10b**) (Ji and Zhao 2015). Compared to simply discarding cases (Zhou et al. 2021), it may be more economical to retain cases by the additional simulation time window given the cost for each impact reconstruction (Sanchez et al. 2018).

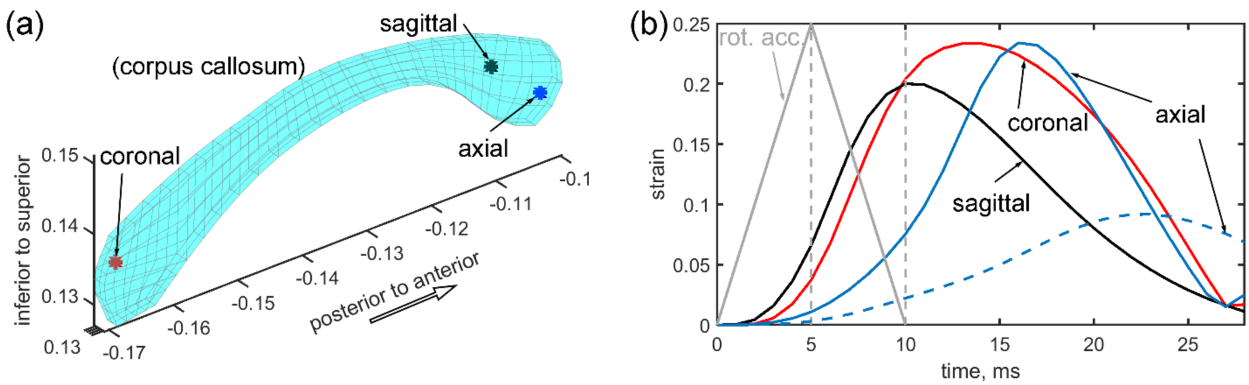

Fig. 10. (**a**) Element locations in the corpus callosum where maxPS occurs during an idealized head rotational acceleration impulse (a triangulated temporal shape with peak magnitude of 4500 rad/s^2 and an impulse duration of 10 ms) along each of the three major axes. (**b**) Normalized head rotational acceleration impulse is compared with the resulting maxPS time histories in the corpus callosum. When the acceleration peak magnitude is reduced to 1500 rad/s^2, maxPS not only reduces the peak value, but also further increases its time-to-peak (dashed line).

Implications

This work contributes towards a comprehensive time-domain characterization of impact-induced dynamic brain strain in the corpus callosum. The resulting correlation with impact rotational peak velocity could allow instantly establishing the strain history to launch multiscale modeling of brain injury deep in the brain. This avoids a costly whole brain model simulation, which would significantly facilitate the exploration of brain injury pathology across length scales in this region.

The rich dynamic information about brain strain also supports further development of advanced deep learning models that will instantly estimate the complete spatiotemporal details of brain strain on a low-end computer. Combining with such a tool, the work presented in this study would set the stage for efficient and large-scale axonal injury model simulations in arbitrary brain regions, including other important white matter areas and the gray-white matter interface (Alisafaei et al. 2020). This may allow translating impact kinematics into the extent of axonal substructural damages (Johnson et al. 2013). The location and extent of these microscopic damages may uncover the pathology of brain injury, beyond statistical correlation commonly used at present for injury prediction that does not infer causation.

Limitations

A limitation of the study is that all results depend on the specific head injury model used, which suffers from any and all limitations with respect to its model assumptions. In particular, a generic WHIM was used for all impact simulations, which did not consider morphological differences such as head size. A larger head/brain would expect to require a longer time lag between kinematics and corpus callosum strain, as similarly found in another study analyzing the whole-brain strain (Liu et al. 2021).

We also purposefully limited our investigation to the mid-sagittal section of the corpus callosum deep in the brain. The surrounding falx and tentorium have important roles in corpus callosum strain (Ho et al. 2017; Hernandez et al. 2019). They were modelled as linear elastic membranes, same as the isotropic KTH (Kleiven 2007), GHBMC (Mao et al. 2013) and another model (Lu et al. 2019), although a hyperelastic model based on more recent experimental data is emerging (Ho et al. 2017; Trotta et al. 2020; Li et al. 2020). In addition, cerebral vasculature also reduces corpus callosum strain (Zhao and Ji 2020b), which is not yet incorporated into the WHIM V1.0 model. It is possible that reanalyzing the results using a different head injury model or an upgraded WHIM V2.1 that embeds cerebral vasculature (Zhao and Ji 2020b, 2022) may change the quantitative results, albeit WHIM V1.0 is similar to other commonly used models when studying whole brain peak maxPS (Fahlstedt et al. 2021). Therefore, we anticipate that at least similar qualitative findings will follow, given that virtually all head injury models adopt viscoelasticity for the brain (Fahlstedt et al. 2021).

The dynamic characteristics for other parts of the brain away from the corpus callosum may be even more complicated, as evident from a recent study showing time histories of maxPS in subcortical regions (Montanino et al. 2021). It does not appear feasible to fit them into idealized peaks. These additional observations on the richness of brain strain dynamics, once again, strongly support the need to further develop advanced deep learning models that will instantly estimate the complete spatiotemporal histories of elementwise brain strains, beyond the spatially detailed peak strains achieved at the maximum value (Ghazi et al. 2021). Dramatically improving head impact simulation efficiency (from hours or days to under a second) could have the potential of transforming acceleration-based TBI studies to focusing on brain strains. This could accelerate new scientific discoveries of TBI biomechanics in the future.

Conclusions

We find that dynamic maximum and minimum principal strains in the corpus callosum can be approximated by Gaussian peaks. The peak magnitudes are significantly correlated with peak impact rotational velocity. These results allow formulating tissue strain dynamics based on impact kinematics directly, without costly impact simulation at the global whole brain level. They can be subsequently used to design *in vitro* neuronal testing protocols and to drive microscale axonal injury model simulations. Extending these findings to real-time macroscopic dynamic simulation of the whole brain could facilitate large- and multi-scale brain injury modeling in arbitrary regions in the future, including the gray-white matter interface. These investigations are expected to enhance the biomechanical characterization and understanding of injury pathology across the length scales. Finally, “features” from dynamic brain strains could improve injury correlation and prediction, but strain time lag relative to kinematics should not be ignored in impact simulation.

Declaration of Competing Interest

The authors declare that they have no known competing financial interests or personal relationships that could have appeared to influence the work reported in this paper.

Acknowledgement

This work is supported by the NIH grant R01 NS092853 and the NSF award under grant No. 2114697. The sponsors do not have any role in the study.

References

Abderezaei J, Zhao W, Grijalva CL, et al (2019) Nonlinear Dynamical Behavior of the Deep White Matter during Head Impact. Phys Rev Appl 12:. https://doi.org/10.1103/PhysRevApplied.12.014058

Ahmadzadeh H, Smith DH, Shenoy VB (2014) Viscoelasticity of tau proteins leads to strain rate-dependent breaking of microtubules during axonal stretch injury: predictions from a mathematical model. Biophys J 106:1123–33. https://doi.org/10.1016/j.bpj.2014.01.024

Alisafaei F, Gong Z, Johnson VE, et al (2020) Mechanisms of Local Stress Amplification in Axons near the Gray-White Matter Interface. Biophys J 1290–1300. https://doi.org/10.1016/j.bpj.2020.08.024

Anderson ED, Giudice JS, Wu T, et al (2020) Predicting Concussion Outcome by Integrating Finite Element Modeling and Network Analysis. Front Bioeng Biotechnol 8:309. https://doi.org/10.3389/fbioe.2020.00309

Bar-Kochba E, Scimone MT, Estrada JB, Franck C (2016) Strain and rate-dependent neuronal injury in a 3D in vitro compression model of traumatic brain injury. Sci Rep 6:1–11. https://doi.org/10.1038/srep30550

Bian K, Mao H (2020) Mechanisms and variances of rotation-induced brain injury: a parametric investigation between head kinematics and brain strain. Biomech Model Mechanobiol 1–19. https://doi.org/10.1007/s10237-020-01341-4

Bigler ED (2016) Systems Biology, Neuroimaging, Neuropsychology, Neuroconnectivity and Traumatic Brain Injury. Front Syst Neurosci 10:1–23. https://doi.org/10.3389/FNSYS.2016.00055

Bigler ED, Maxwell WL (2012) Neuropathology of mild traumatic brain injury: Relationship to neuroimaging findings. Brain Imaging Behav 6:108–136. https://doi.org/10.1007/s11682-011-9145-0

Escarcega JD, Knutsen AK, Okamoto RJ, et al (2021) Natural oscillatory modes of 3D deformation of the human brain in vivo. J Biomech 119:110259. https://doi.org/10.1016/j.jbiomech.2021.110259

Fahlstedt M, Abayazid F, Panzer MB, et al (2021) Ranking and Rating Bicycle Helmet Safety Performance in Oblique Impacts Using Eight Different Brain Injury Models. Ann Biomed Eng 1–13. https://doi.org/10.1007/s10439-020-02703-w

Gabler LF, Crandall JR, Panzer MB (2018) Development of a Metric for Predicting Brain Strain Responses Using Head Kinematics. Ann Biomed Eng 46:1–14. https://doi.org/10.1007/s10439-018-2015-9

Garimella HT, Menghani RR, Gerber JI, et al (2019) Embedded Finite Elements for Modeling Axonal Injury. Ann Biomed Eng 47:1–19. https://doi.org/10.1007/s10439-018-02166-0

Ghazi K, Wu S, Zhao W, Ji S (2021) Instantaneous Whole-Brain Strain Estimation in Dynamic Head Impact. J Neurotrauma 38:1023–1035. https://doi.org/10.1089/neu.2020.7281

Giordano C, Kleiven S (2014) Evaluation of Axonal Strain as a Predictor for Mild Traumatic Brain Injuries Using Finite Element Modeling. Stapp Car Crash J 58:29–61. https://doi.org/10.4271/2014-22-0002

Hernandez F, Giordano C, Goubran M, et al (2019) Lateral impacts correlate with falx cerebri displacement and corpus callosum trauma in sports-related concussions. Biomech Model Mechanobiol 1–19. https://doi.org/10.1007/s10237-018-01106-0

Hernandez F, Wu LC, Yip MC, et al (2015) Six Degree-of-Freedom Measurements of Human Mild Traumatic Brain Injury. Ann Biomed Eng 43:1918–1934. https://doi.org/10.1007/s10439-014-1212-4

Ho J, Zhou Z, Li X, Kleiven S (2017) The peculiar properties of the falx and tentorium in brain injury biomechanics. J Biomech 60:243–247. https://doi.org/10.1016/j.jbiomech.2017.06.023

Ji S, Zhao W (2015) A Pre-computed Brain Response Atlas for Instantaneous Strain Estimation in Contact Sports. Ann Biomed Eng 43:1877–1895. https://doi.org/10.1007/s10439-014-1193-3

Ji S, Zhao W (2022) Displacement voxelization to resolve mesh-image mismatch: application in deriving dense white matter fiber strains. Comput Methods Programs Biomed 213:106528. https://doi.org/10.1016/j.cmpb.2021.106528

Ji S, Zhao W, Ford JC, et al (2015) Group-wise evaluation and comparison of white matter fiber strain and maximum principal strain in sports-related concussion. J Neurotrauma 32:441–454. https://doi.org/10.1089/neu.2013.3268

Ji S, Zhao W, Li Z, McAllister TW (2014) Head impact accelerations for brain strain-related responses in contact sports: a model-based investigation. Biomech Model Mechanobiol 13:1121–36. https://doi.org/10.1007/s10237-014-0562-z

Johnson VE, Stewart W, Smith DHDH (2013) Axonal pathology in traumatic brain injury. Exp Neurol 246:35–43. https://doi.org/10.1016/j.expneurol.2012.01.013

Kalambet Y, Kozmin Y, Mikhailova K, et al (2011) Reconstruction of chromatographic peaks using the exponentially modified Gaussian function. J Chemom 25:352–356. https://doi.org/10.1002/cem.1343

Kenzie ES, Parks EL, Bigler ED, et al (2017) Concussion as a multi-scale complex system: An interdisciplinary synthesis of current knowledge. Front. Neurol. 8:1

King AI, Yang KH, Zhang L, et al (2003) Is head injury caused by linear or angular acceleration? In: IRCOBI Conference. Lisbon, Portugal, Portugal, pp 1–12

Kleiven S (2007) Predictors for Traumatic Brain Injuries Evaluated through Accident Reconstructions. Stapp Car Crash J 51:81–114. https://doi.org/2007-22-0003 [pii]

Kleiven S, Hardy WNW (2002) Correlation of an FE model of the human head with local brain motion – Consequences for injury prediction. Stapp Car Crash J 46:123–144. https://doi.org/2002-22-0007 [pii]

Laksari K, Wu LC, Kuo C, et al (2015) Resonance of human brain under head acceleration. J R Soc Interface 12:20150331. https://doi.org/10.1098/rsif.2015.0331

Li X, Zhou Z, Kleiven S (2020) An anatomically accurate and personalizable head injury model: Significance of brain and white matter tract morphological variability on strain. Biomech Model Mechanobiol 1–29. https://doi.org/10.1101/2020.05.20.105635

Liu Y, Domel AG, Cecchi NJ, et al (2021) Time Window of Head Impact Kinematics Measurement for Calculation of Brain Strain and Strain Rate in American Football. Ann Biomed Eng 1–14. https://doi.org/10.1007/s10439-021-02821-z

Liu Y, Domel AG, Yousefsani SA, et al (2020) Validation and Comparison of Instrumented

Mouthguards for Measuring Head Kinematics and Assessing Brain Deformation in Football Impacts. Ann Biomed Eng 48:2580–2598. https://doi.org/10.1007/s10439-020-02629-3

Lu YC, Daphalapurkar NP, Knutsen AK, et al (2019) A 3D Computational Head Model Under Dynamic Head Rotation and Head Extension Validated Using Live Human Brain Data, Including the Falx and the Tentorium. Ann Biomed Eng 47:1923–1940. https://doi.org/10.1007/s10439-019-02226-z

Mao H, Zhang L, Jiang B, et al (2013) Development of a finite element human head model partially validated with thirty five experimental cases. J Biomech Eng 135:111002–15. https://doi.org/10.1115/1.4025101

Marklund N, Hillered L (2011) Animal modelling of traumatic brain injury in preclinical drug development: where do we go from here? Br J Pharmacol 164:1207–29. https://doi.org/10.1111/j.1476-5381.2010.01163.x

McAllister TW, Ford JC, Ji S, et al (2012) Maximum principal strain and strain rate associated with concussion diagnosis correlates with changes in corpus callosum white matter indices. Ann Biomed Eng 40:127–40. https://doi.org/10.1007/s10439-011-0402-6

Meaney DF, Morrison B, Bass CR (2014) The Mechanics of Traumatic Brain Injury: A Review of What We Know and What We Need to Know for Reducing Its Societal Burden. J Biomech Eng 136:. https://doi.org/10.1115/1.4026364

Miller LE, Urban JE, Davenport EM, et al (2021) Brain Strain: Computational Model-Based Metrics for Head Impact Exposure and Injury Correlation. Ann Biomed Eng 49:1083–1096. https://doi.org/10.1007/s10439-020-02685-9

Mittermayr CR, Nikolov SG, Hutter H, Grasserbauer M (1996) Wavelet denoising of Gaussian peaks: A comparative study. Chemom Intell Lab Syst 34:187–202. https://doi.org/10.1016/0169-7439(96)00026-3

Mojahed A, Abderezaei J, Kurt M, et al (2020) A Nonlinear Reduced-Order Model of Corpus Callosum Under Coronal Excitation. J Biomech Eng 142:. https://doi.org/10.1115/1.4046503

Montanino A, Li X, Zhou Z, et al (2021) Subject-specific multiscale analysis of concussion: from macroscopic loads to molecular-level damage. Brain Multiphysics 100027. https://doi.org/10.1016/j.brain.2021.100027

Montanino A, Saeedimasine M, Villa A, Kleiven S (2019) Axons Embedded in a Tissue May Withstand Larger Deformations Than Isolated Axons Before Mechanoporation Occurs. J Biomech Eng 141:. https://doi.org/10.1115/1.4044953

Morrison B, Elkin BS, Dollé J-P, Yarmush ML (2011) In vitro models of traumatic brain injury. Annu Rev Biomed Eng 13:91–126. https://doi.org/10.1146/annurev-bioeng-071910-124706

O'Haver T (2021) peakfit.m (https://www.mathworks.com/matlabcentral/fileexchange/23611-peakfit-m), MATLAB Central File Exchange. Retrieved June 10, 2021.

Post A, Hoshizaki T, Gilchrist M, Cusimano M (2017) Peak linear and rotational acceleration magnitude and duration effects on maximum principal strain in the corpus callosum for sport impacts. J Biomech 61:183–192

Sahoo D, Deck C, Willinger R (2016) Brain injury tolerance limit based on computation of axonal strain. Accid Anal Prev 92:53–70. https://doi.org/10.1016/j.aap.2016.03.013

Sanchez EJ, Gabler LF, Good AB, et al (2018) A reanalysis of football impact reconstructions for head kinematics and finite element modeling. Clin Biomech 64:82–89. https://doi.org/10.1016/j.clinbiomech.2018.02.019

Shakiba D, Zhao W, Ji S (2020) Multiscale Mechanobiology of Brain Injury: Axonal Strain Redistribution. Biophys J 1–2. https://doi.org/10.1016/j.bpj.2020.07.041

Trotta A, Clark JM, McGoldrick A, et al (2020) Biofidelic Finite Element Modelling of Brain Trauma: Importance of the Scalp in Simulating Head Impact. Int J Mech Sci 173:105448. https://doi.org/10.1016/j.ijmecsci.2020.105448

Viano DC, Casson IR, Pellman EJ, et al (2005) Concussion in professional football: Brain responses by finite element analysis: Part 9. Neurosurgery 57:891–915. https://doi.org/10.1227/01.NEU.0000186950.54075.3B

Wahab MF, O'Haver TC (2020) Wavelet transforms in separation science for denoising and peak overlap detection. J Sep Sci 43:1998–2010. https://doi.org/10.1002/jssc.202000013

Wu S, Zhao W, Ghazi K, Ji S (2019a) Convolutional neural network for efficient estimation of regional brain strains. Sci Rep 9:17326: https://doi.org/https://doi.org/10.1038/s41598-019-53551-1

Wu S, Zhao W, Rowson B, et al (2020) A network-based response feature matrix as a brain injury metric. Biomech Model Mechanobiol 19:927–942. https://doi.org/https://doi.org/10.1007/s10237-019-01261-y

Wu S, Zhao W, Ruan J, et al (2021) Instantaneous brain strain estimation for automotive head impacts via deep learning. Stapp Car Crash J 65:

Wu T, Alshareef A, Giudice JS, Panzer MB (2019b) Explicit Modeling of White Matter Axonal Fiber Tracts in a Finite Element Brain Model. Ann Biomed Eng 1–15. https://doi.org/10.1007/s10439-019-02239-8

Zhao W, Bartsch A, Benzel E, et al (2019) Regional Brain Injury Vulnerability in Football from Two Finite Element Models of the Human Head. In: IRCOBI. Florence, Italy, pp 619–621

Zhao W, Cai Y, Li Z, Ji S (2017) Injury prediction and vulnerability assessment using strain and susceptibility measures of the deep white matter. Biomech Model Mechanobiol 16:1709–1727. https://doi.org/10.1007/s10237-017-0915-5

Zhao W, Ji S (2019) White matter anisotropy for impact simulation and response sampling in traumatic brain injury. J Neurotrauma 36:250–263. https://doi.org/10.1089/neu.2018.5634

Zhao W, Ji S (2020a) Displacement- and strain-based discrimination of head injury models across a wide range of blunt conditions. Ann Biomed Eng 20:1661–1677. https://doi.org/10.1007/s10439-020-02496-y

Zhao W, Ji S (2020b) Incorporation of vasculature in a head injury model lowers local mechanical strains in dynamic impact. J Biomech 104:109732

Zhao W, Ji S (2022) Cerebral vascular strains in dynamic head impact using an upgraded model with brain material property heterogeneity. J Mech Behav Biomed Mater 126:104967. https://doi.org/10.1016/j.jmbbm.2021.104967

Zhao W, Wu Z, Ji S (2021) Displacement Error Propagation From Embedded Markers to Brain Strain. J Biomech Eng 143:1–10. https://doi.org/10.1115/1.4051050

Zhou Z, Li X, Liu Y, et al (2021) Toward a Comprehensive Delineation of White Matter Tract-Related Deformation. J Neurotrauma 38:3260–3278. https://doi.org/10.1089/neu.2021.0195